

## Interleukin-30 Promotes Breast Cancer Growth and Progression

Irma Airoidi<sup>1</sup>, Claudia Cocco<sup>1</sup>, Carlo Sorrentino<sup>2,3</sup>, Domenico Angelucci<sup>4</sup>, Serena Di Meo<sup>2,3</sup>, Lamberto Manzoli<sup>5</sup>, Silvia Esposito<sup>2,3</sup>, Domenico Ribatti<sup>6</sup>, Maria Bertolotto<sup>7</sup>, Laura Iezzi<sup>8</sup>, Clara Natoli<sup>8</sup>, and Emma Di Carlo<sup>2,3</sup>

### Abstract

The inflammatory tissue microenvironment that promotes the development of breast cancer is not fully understood. Here we report a role for elevated IL30 in supporting the breast cancer cell viability and invasive migration. IL30 was absent in normal mammary ducts, ductules, and acini of histologically normal breast and scanty in the few stromal infiltrating leukocytes. In contrast, IL30 was expressed frequently in breast cancer specimens where it was associated with triple-negative and HER2<sup>+</sup> molecular subtypes. In stromal leukocytes found in primary tumors or tumor-draining lymph nodes, which included mainly CD14<sup>+</sup> monocytes, CD68<sup>+</sup> macrophages, and CD33<sup>+</sup>/CD11b<sup>+</sup> myeloid cells, IL30 levels increased with disease stage and correlated with recurrence. A negative correlation was determined between IL30 expression by nodal stromal leukocytes and overall survival. *In vitro* studies showed that

human recombinant IL30 upregulated expression of a pro-oncogenic program, including especially IL6 in both triple-negative and HER2<sup>+</sup> breast cancer cells. In triple-negative breast cancer cells, IL30 boosted a broader program of proliferation, invasive migration, and an inflammatory milieu associated with KISS1-dependent metastasis. Silencing of STAT1/STAT3 signaling hindered the regulation of the primary growth and progression factors in breast cancer cells. IL30 administration *in vivo* fostered the growth of triple-negative breast cancer by promoting proliferation and vascular dissemination of cancer cells and the accumulation of intratumoral CD11b<sup>+</sup>/Gr1<sup>+</sup> myeloid cell infiltrates. Overall, our results show how IL30 regulates breast cancer cell viability, migration, and gene expression to promote breast cancer growth and progression and its impact on patient outcome. *Cancer Res*; 76(21); 6218–29. ©2016 AACR.

### Introduction

Breast cancer is a leading cause of cancer death in women worldwide (1). Its molecular signature has profound clinical implications (2), but a critical role has also been established for the microenvironment in disease progression (3). Microenvironmental signals and molecular alterations of cancer may condition each other and have an impact on tumor behavior (3).

In an attempt to decipher messages released within the breast cancer microenvironment, we ran into the endogenous expression of a newly discovered cytokine known as IL30.

Identified as p28, a polypeptide related to IL12A (IL12p35; ref. 4), IL30 can bind Epstein–Barr virus–induced 3 (EBI3) to form IL27, which has revealed antitumor effects in several models (5, 6), but it also acts as a self-standing cytokine with its own functional properties (7). It has been shown to bind to, but not signal via, the receptor (R) chain gp130, thereby antagonizing signaling via the receptors for IL6 and IL27, resulting in anti-inflammatory effects (8), but also to signal via IL6R by recruiting a gp130 homodimer, behaving similarly to IL6 and IL11 and thus endowed with proinflammatory potential (9). The immunologic functions of IL30 are thus complex and currently under active investigation, whereas its role in cancer biology is mostly unknown. As a matter of fact, IL30 has been ascribed with a tumor-promoting potential. It was shown to suppress the anti-tumor effects of IL27 in colon cancer and to reduce the survival of colon cancer-bearing mice (10). Recently, we have provided evidences that IL30 supports proliferation and gene expression alteration in prostate cancer cells and that IL30 expression in the prostate and draining lymph nodes from patients with prostate cancer is associated with poorly differentiated, high-grade tumor and metastatic stage of disease (11, 12).

To answer the question of whether IL30 has a role in breast cancer, we investigated its expression in breast and axillary nodes from patients with different molecular classes of breast cancers and correlated molecular data with clinical–pathologic parameters. Results from *in vitro* and *in vivo* experiments shed a light

<sup>1</sup>Laboratorio di Oncologia, Istituto Giannina Gaslini, Genova, Italy. <sup>2</sup>Department of Medicine and Sciences of Aging, Division of Anatomic Pathology and Molecular Medicine, "G. d'Annunzio" University, Chieti, Italy. <sup>3</sup>Ce.S.I.-MeT, Aging Research Center, "G. d'Annunzio" University, Chieti, Italy. <sup>4</sup>Division of Pathology, "SS. Annunziata Hospital", Chieti, Italy. <sup>5</sup>Department of Medicine and Sciences of Aging, "G. d'Annunzio" University, Chieti, Italy. <sup>6</sup>Department of Basic Medical Sciences, Neurosciences and Sensory Organs, University of Bari Medical School, and National Cancer Institute "Giovanni Paolo II", Bari, Italy. <sup>7</sup>Laboratory of Phagocyte Physiopathology and Inflammation, Department of Internal Medicine, University of Genova, Genova, Italy. <sup>8</sup>Department of Medical, Oral and Biotechnological Sciences, "G. d'Annunzio" University, Chieti, Italy.

**Note:** Supplementary data for this article are available at Cancer Research Online (<http://cancerres.aacrjournals.org/>).

I. Airoidi and C. Cocco have contributed equally to this study.

**Corresponding Author:** Emma Di Carlo, Department of Medicine and Sciences of Aging, Division of Anatomic Pathology and Molecular Medicine, "G. d'Annunzio" University, "SS Annunziata" Hospital, Via dei Vestini, Chieti 66100, Italy. Phone: 39-0871-357395; Fax: 39-0871-540079; E-mail: edicarlo@unich.it

**doi:** 10.1158/0008-5472.CAN-16-0189

©2016 American Association for Cancer Research.

on the mechanisms underlying the implication of IL30 in breast cancer development and progression.

## Materials and Methods

### Ethics statement

Animal experiments were performed according to the Italian Legislative Order January 27, 1992, n.116, and the EC Directive 86/609, OJL 358, December 1, 1987. Written informed consent was obtained from patients. The study was performed in accordance with the principles outlined in the Declaration of Helsinki and approved by the Ethical Committee of the "G. d'Annunzio" University and Local-Health-Authority of Chieti, Italy.

### Patients and samples

Normal and malignant breast samples and axillary lymph nodes came from 156 untreated women who underwent surgery for breast cancer at the "SS. Annunziata Hospital", Chieti, between June 1, 2000 and November 31, 2011. Breast cancer molecular subtypes were classified according to the St. Gallen International Expert Consensus as follows: luminal A [estrogen receptor (ER)<sup>+</sup> and/or progesterone receptor (PR)<sup>+</sup> and Ki-67 < 20%]; luminal B (ER<sup>+</sup> and/or PR<sup>+</sup>, which can be further distinguished in Ki-67 ≥ 20%, or HER2<sup>+</sup> tumors); HER2<sup>+</sup> (ER<sup>-</sup>, PR<sup>-</sup>, and HER2<sup>+</sup>); triple-negative (ER<sup>-</sup>, PR<sup>-</sup>, and HER2<sup>-</sup>). Patients' clinical-pathological characteristics are shown in Table 1. Details on sample collection and processing are provided in the Supplementary Methods.

### Cell culture, flow cytometry, and MTT assay

MDA-MB-231, SK-BR-3, MDA-MB-361, and T47D cells were from the ATCC, which performed their characterizations by short tandem repeats profile analysis. The cells were passaged for fewer than 6 months after resuscitation. MDA-MB-231 and SK-BR-3 were cultured in RPMI-1640, 10% FCS. MDA-MB-361 and T47D were cultured in DMEM low glucose, 10% FCS. hrIL30 (IL27p28, Abnova) was used at 200 ng/mL, following titration experiments using 10 to 200 ng/mL. IL30R expression, apoptosis, and proliferation in human (h) breast cancer (BRCA) cells were assessed as described in the Supplementary Methods.

### STAT1 and STAT3 knockdown

Silencing of *STAT1* and *STAT3*, in MDA-MB-231 cells, was performed using the FlexiTube GeneSolution (Qiagen). Two siRNAs, for each transcription factor, with the highest knockdown efficiency, were selected, as reported in the Supplementary Methods.

### Migration and invasion assays

CytoSelect Cell Migration and Invasion Assay Kit (Cell Biolabs) was used as described in the Supplementary Methods.

### Real-time RT-PCR and PCR arrays

The real-time RT-PCR was carried out on human breast tissues and on IL30-treated and untreated hBRCA cell lines, as described in the Supplementary Methods.

### Western blotting

Western blotting was performed to assess *STAT1* and *STAT3* knockdown in MDA-MB-231 cells, as described in the Supplementary Methods.

### Mouse studies

The optimal conditions for *in vivo* studies were assessed as described in the Supplementary Methods. Two groups of 8 animals were subcutaneously injected unilaterally with  $1.5 \times 10^6$  MDA-MB-231 cells in the fourth abdominal fat pad. One group was treated subcutaneously with biweekly doses of hrIL30 (1 µg dose/mouse), starting 2 days after tumor cell inoculation. The control group was treated with PBS according to the same schedule. The mice were sacrificed at day 19, when signs of poor health became evident. Tumor masses were removed and measured and then formalin-fixed or snap-frozen for histopathologic analyses.

### Immunohistochemistry

Immunohistochemical analysis was performed as described in the Supplementary Methods, using the antibodies listed in the Supplementary Table S1. Double and triple immunohistochemistry was performed as reported (11). Proliferation index, microvessel, and immune cell counts were assessed at 400× in a 0.180-µm<sup>2</sup> field. At least 3 samples (3 sections per sample) and 6 to 8 randomly chosen fields per section were evaluated. Results are expressed as mean ± SD of positive cells per field (or Ki-67-positive cells per number of total cells) evaluated on paraffin-embedded (Ki-67, CD11b/Gr1) or frozen (CD31, Ly6G, Mac-1, Asialo GM1) sections by immunohistochemistry.

### Morphometric analyses

IL30 expression by primary tumours (T) or lymph node metastases was evaluated according to the following criteria: (i) the widening of the staining expressed as the percentage of tumor or metastasis stained that is, <50%, ≥50% ≤ 70%, and >70% and (ii) the strength of the staining defined as absent (-), slight (±), distinct (+), or strong (++).

Thus, IL30 immunostaining was defined as positive, weakly positive, or negative, as specified in the Supplementary Methods.

Tumor (T)-infiltrating leukocytes (ILK) or lymph node (LN)-ILK expression of IL30 was evaluated using the following score on the basis of (i) the percentage of leukocyte expressing the cytokine, that is, <50%, ≥ 50% ≤ 70% and > 70% and (ii) the

**Table 1.** Characteristics and outcomes of the sample

	Overall sample (N = 156)
<b>Baseline characteristics</b>	
Mean age (SD), y	59.0 (11.5)
Histotypes, %	
Ductal carcinoma	39.7
Lobular carcinoma	16.7
Others	43.6
Molecular classes, %	
HER2 <sup>+</sup>	17.9
Luminal A	31.4
Luminal B	35.9
Triple-negative	14.7
HER2 expression, %	32.0
Stage, %	
IA	37.8
IIA or IIB	28.2
IIIA or IIIB or IIIC	34.0
Lymph node metastases, %	51.9
<b>Outcomes</b>	
Mean follow-up duration (SD), y	6.8 (2.5)
Cancer relapse, %	35.9
Death, %	26.9

strength of the cytokine staining, which was defined as absent (-), scarce ( $\pm$ ), distinct (+), or strong (++)

Thus, IL30 expression by T-ILK or LN-ILK was defined as strong, distinct, or scanty, as specified in the Supplementary Methods

The immunostained sections were examined by 2 pathologists with very good agreement ( $\kappa = 0.82, 0.75,$  and  $0.79$  for evaluations of IL30 staining in T, T-ILK, or LN-ILK, respectively).

**Statistical analysis**

The levels of IL30 expression were determined: (i) in tumor cells of breast cancers; (ii) in T-ILK; and (iii) in LN-ILK. We evaluated the potential association between each of the 3 measures of IL30 expression with all the other baseline variables using Fisher exact test for categorical variables and *t* test for continuous ones. The potential association between IL30 levels and cancer recurrence or death during the follow-up was investigated as described in the Supplementary Methods.

Tumor volumes were reported in  $\text{mm}^3$  versus time. Differences in tumor volume, proliferation index, microvessel density, and counts of immune cells between tumors from hrIL30- and PBS-treated mice were assessed by Student *t* test, and data were reported as mean  $\pm$  SD. The SPSS software, version 11.0 (IBM) was employed, with  $P < 0.05$  as the significance cutoff.

**Results**

**IL30 expression by breast cancer and BRCA-ILK is associated with triple-negative and HER2<sup>+</sup> tumors**

To assess whether the breast cancer microenvironment might be characterized by IL30 expression, we first performed immunohistochemical analyses of breast tissues and axillary lymph nodes from 156 untreated women who underwent surgery for breast cancer (Table 1) and from control subjects, by using a mAb specific against the p28 subunit of IL27. IL30 was absent in normal mammary ducts, ductules, and acini of histologically normal breast samples (from both patients with

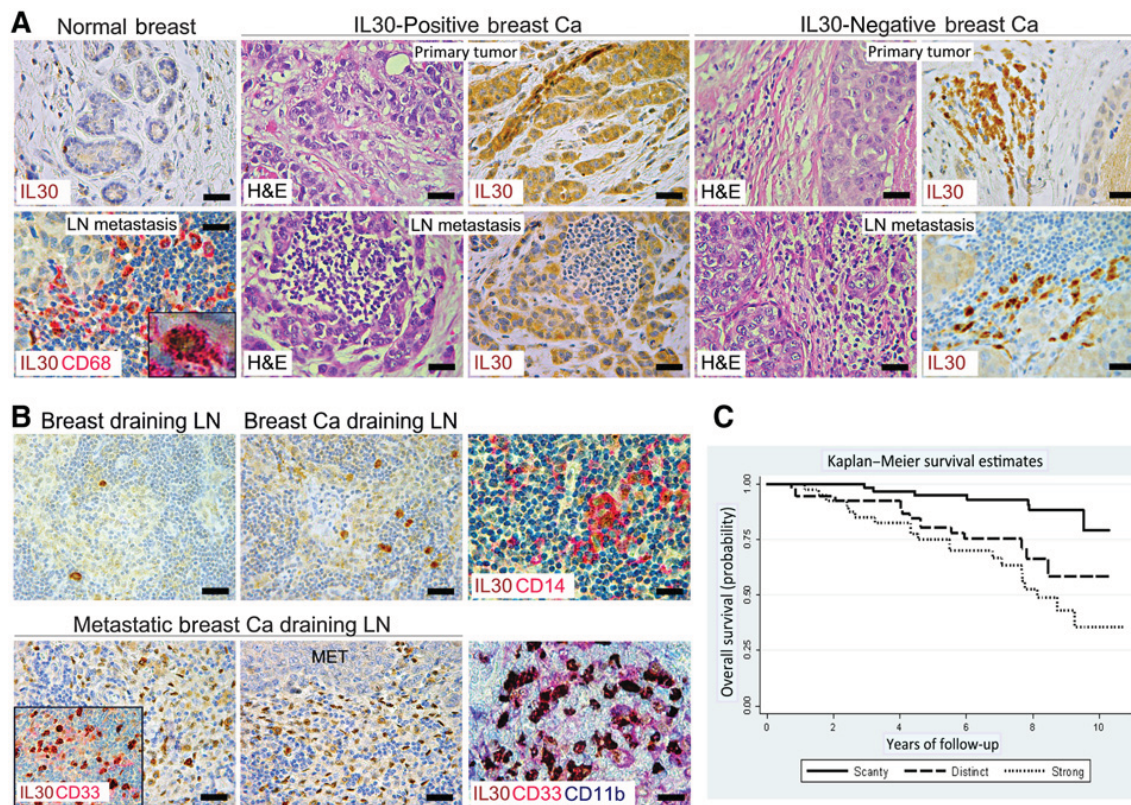


**Figure 1.** Expression of IL30 in breast tissue and draining lymph nodes. **A**, IL30 (brown) was almost absent in normal breast tissue, whereas it was expressed in breast cancer (HER2<sup>+</sup> ductal carcinoma) by cancer cells (top middle) or by ILK (triple-negative ductal carcinoma; top right) and in their lymph node metastasis by cancer cells (bottom middle) or ILK (bottom right), mainly identifiable as CD68<sup>+</sup> macrophages (red; bottom left) shown at  $\times 1,000$ , in the inset ( $\times 400$ ). H&E, hematoxylin and eosin. Scale bars, 30  $\mu\text{m}$ . **B**, IL30 expression was scanty in normal breast draining lymph nodes, scanty to distinct in lymph nodes draining breast cancer stage IA, whereas it was strong in lymph nodes, with or without metastasis (MET), draining breast cancer stage IIIA. Expression of IL30 (brown) in the lymph nodes draining metastatic breast cancer, colocalized with CD14<sup>+</sup> cells (red; top right), and mainly with CD33<sup>+</sup> cells (red; inset in the bottom left), most of which coexpressed CD11b (blue), as shown in brick red (bottom right,  $\times 630; \times 400$ ). Scale bars, 20  $\mu\text{m}$  (bottom right); 30  $\mu\text{m}$  (the remaining panels). **C**, Kaplan–Meier estimates for all stages of patients with breast cancer ( $n = 156$ ) classified by level of IL30 expression in LN-ILK, "scanty" ( $n = 63$ ), "distinct" ( $n = 53$ ), and "strong" ( $n = 40$ ).

breast cancer and controls) and scanty in the few stromal ILK. In contrast, IL30 expression was frequent (ranging from positive to weakly positive) in the neoplastic epithelia of the majority (114 of 156; 73%) of breast cancers (Fig. 1A, Supplementary Table S2) with confirmation at the transcriptional level by real-time RT-PCR.

IL30 expression by the neoplastic epithelial component of the primary tumors involved most of the tumors belonging to the poorer prognosis molecular classes, specifically 89.3% of the HER2<sup>+</sup> and 87.0% of triple-negative subtypes. In contrast, Fisher exact test revealed that the luminal A subtype included a significantly lower percentage of IL30-positive breast cancers (61.2%). Taken as a whole, the HER2<sup>+</sup> breast cancers (which include those belonging to HER2<sup>+</sup> class and the luminal B HER2<sup>+</sup> subtype) include a significantly ( $P < 0.05$ ) higher percentage of IL30-positive tumors (84%) than the HER2<sup>-</sup> breast cancers (67.9%; Supplementary Table S2).

A distinct to strong IL30 expression in BRCA-ILK, mostly represented by CD68<sup>+</sup> macrophages, CD14<sup>+</sup> monocytes, and CD33<sup>+</sup> myeloid cells, involved 73 of 156, that is, 46.7%, of all breast cancers (Fig. 1A, Supplementary Table S3), most of them belonging to triple-negative or HER2<sup>+</sup> subtypes. A significant difference ( $P < 0.05$ ) was disclosed in the percentage of tumors endowed with a distinct to strong expression of IL30 by BRCA-ILK between the triple-negative (65.2%) or HER2<sup>+</sup> (64.3%) breast cancers and the luminal A subtype (30.6%). The vast majority (69.4%) of breast cancers included in this molecular class was characterized by a scanty leukocyte expression of IL30, which was comparable to that observed in normal breast tissues (Supplementary Table S3).

#### IL30 expression by leukocytes infiltrating breast cancer and draining lymph nodes correlates with the stage of disease

The proportion of breast cancers infiltrated by IL30-expressing leukocytes increased with the stage of disease. IL30 expression increased significantly ( $P < 0.05$ ) in stage II versus stage I and in stage III versus stage I, which mostly included tumors (67.8%, Supplementary Table S3) and draining nodes (62.7%, Table 2) endowed with a scanty IL30 expression by infiltrating leukocytes, which was comparable to that observed in normal breast and control lymph node tissues. Moreover, in multivariable analysis, a significant association was disclosed between IL30 expression by both BRCA-ILK and LN-ILK and disease stage (Supplementary Table S4). Interestingly, a distinct-to-strong leukocyte expression of IL30, in both primary tumor and draining lymph nodes, was significantly ( $P < 0.001$ ) associated with the presence of lymph node metastasis (Fig. 1A, Supplementary Table S3, and Table 2). IL30 production, which mostly colocalized with CD68<sup>+</sup> macrophages, CD14<sup>+</sup> monocytes, and CD33<sup>+</sup>/CD11b<sup>+</sup> myeloid cells, was wider and stronger in the lymphatic sinuses of lymph nodes draining metastatic breast cancer, whether they harbor the metastasis or simply drain the metastatic tumor, than in lymph nodes draining nonmetastatic BRCA (of any stage) or in control nodes (Fig. 1B).

#### Expression of IL30 in breast cancer draining lymph nodes is associated with disease recurrence and correlates with mortality at the multivariate analysis

Univariate analyses revealed that high level (ranging from distinct to strong) of IL30 expression by LN-ILK was significantly ( $P < 0.001$ ) associated with disease recurrence, as 80.4%

**Table 2.** Characteristics and outcomes by levels of IL30 expression in leukocytes infiltrating lymph nodes

	IL30 expression				<i>P</i> <sup>a</sup>
	Scanty ( <i>n</i> = 63)	Distinct ( <i>n</i> = 53)	Strong ( <i>n</i> = 40)	Distinct or strong ( <i>n</i> = 93)	
Mean age (SD), y	55.8 (9.7)	62.0 (12.4)	60.2 (11.8)	61.2 (12.1)	0.004
Histotypes, %					
Ductal carcinoma	40.3	30.7	29.0	59.7	
Lobular carcinoma	42.3	46.2	11.5	57.7	
Others	39.7	32.4	27.9	60.3	
Molecular classes, %					
Luminal A	46.9	32.7	20.4	53.1	
Luminal B	41.1	30.4	28.6	58.9	
HER2 <sup>+</sup>	35.7	32.1	32.1	64.3	
Triple-negative	30.4	47.8	21.7	69.6	
HER2 expression, %					
HER2 <sup>-</sup>	45.3	31.1	23.6	54.7	
HER2 <sup>+</sup>	30.0	40.0	30.0	70.0	
Stage, %					
IA	62.7	32.2	5.1	37.3	
IIA or IIB	36.4	29.6	34.1	63.6	<0.05 <sup>b</sup>
IIIA or IIIB or IIIC	18.9	39.6	41.5	81.1	<0.05 <sup>b</sup>
Lymph node metastases, %					<0.001
No	62.7	29.3	8.0	37.3	
Yes	19.8	38.3	42.0	80.3	
<b>Outcomes</b>					
Mean follow-up duration (SD), y	7.4 (2.1)	6.2 (2.4)	6.6 (2.9)	6.4 (2.6)	
Cancer recurrence, %					<0.001
No	52.0	32.0	16.0	48.0	
Yes	19.6	37.5	42.9	80.4	
Death, %					<0.001
No	49.1	33.3	17.5	50.9	
Yes	16.7	35.7	47.6	83.3	

NOTE: Nonsignificant *P* values have not been reported.

<sup>a</sup>Fisher exact test for categorical variables; *t* test for continuous ones.

<sup>b</sup>Versus Stage IA.

(45 of 56) of relapsing patients had high levels of IL30 expression in their cancer draining axillary lymph nodes. Furthermore, 83.3% (35 of 42) of patients who died from cancer had elevated IL30 expression levels in their cancer draining lymph nodes. In Kaplan–Meier survival curves, the overall survival probability gradually decreased when IL30 expression by LN-ILK progressed from scanty, distinct to strong (Fig. 1C). The difference between the overall time of survival of patients with scanty versus distinct or strong IL30 expression by LN-ILK was significant at log-rank test ( $P < 0.001$ ). The Cox proportional hazard model, adjusted for age, histotype, molecular class, HER2 expression, stage, and lymph node metastasis, showed a significant association between a strong IL30 expression by LN-ILK and breast cancer–related mortality [adjusted HR, 2.52; 95% confidence interval (CI), 1.03–6.13; Table 3].

### Triple-negative and HER2<sup>+</sup> breast cancer cell lines express IL30R and IL30 treatment regulates their expression of breast cancer–associated genes

To investigate the effects of IL30 on breast cancer cells, we first tested by flow cytometry the expression of gp130 and IL6R $\alpha$ , the two IL30 receptor chains, in cell lines representative of the major breast cancer subtypes. MDA-MB-231 (triple-negative), SK-BR-3 (HER2<sup>+</sup>), MDA-MB-361 (luminal B HER2<sup>+</sup>), T47D (luminal A) cells expressed both receptor chains, although at different levels (Fig. 2A). MDA-MB-231 cells were 86% gp130<sup>+</sup> and 98% IL6R $\alpha$ <sup>+</sup>, SK-BR-3 cells were

90% gp130<sup>+</sup> and 99% IL6R $\alpha$ <sup>+</sup>, MDA-MB-361 cells were 24% gp130<sup>+</sup> and 99% IL6R $\alpha$ <sup>+</sup>, T47D cells were 65% gp130<sup>+</sup> and 99% IL6R $\alpha$ <sup>+</sup>. Because of their highest expression of both IL30R chains, we then selected MDA-MB-231 (triple-negative) and SK-BR-3 (HER2<sup>+</sup>) cell lines for subsequent *in vitro* experiments.

MDA-MB-231 and SK-BR-3 cells were cultured in the presence or absence of hrIL30, at different time points, and tested for proliferation and apoptosis. IL30 was ineffective on tumor cell survival but increased proliferation particularly in MDA-MB-231 cells, which revealed a significant ( $P < 0.05$ ) proliferative response, by MTT assay, starting from 48-hour treatment with 200 ng/mL of cytokine (Fig. 2B). We then assessed the ability of IL30 to regulate, in both cell lines, the expression of breast cancer–associated genes. Breast cancer PCR-Array (Fig. 2C) revealed that hrIL30 significantly upregulated, in both MDA-MB-231 and SK-BR-3 cells, the proto-oncogenes MYC (3.64 and 5.49 times) and MUC1 (3.32 and 4.98 times), along with genes coding for growth factors such as EGF (7.29 and 4.97 times) and VEGF-A (8.46 and 5.72 times), and the proinflammatory cytokine IL6 (19.23 and 5.57 times), but it also upregulated some tumor suppressor genes, namely CDKN1A/p21 (12.84 and 3.16 times, respectively; ref. 13), CDKN1C/p57 (3.85 and 5.97 times; ref. 14), and CDH13 (4.72 and 3.72 times; ref. 15). Other genes were differently regulated by IL30 in the 2 cell lines. In particular, ADAM23, APC, CCNA1, CDKN2A, CTNNA1, GSTP1, ID1, KRT18, MAPK8, MKI67, MMP9, NME1, XBP1, RB1, SLC39A6, and PTEN were upregulated only in SK-BR-3 cells, whereas in MDA-MB-231 cells,

**Table 3.** Crude and adjusted HR of breast cancer recurrence and related death by each variable in Cox proportional hazard models

	Cancer recurrence			Death		
	Crude HR (95% CI)	Adjusted HR <sup>a</sup> (95% CI)	P <sup>a</sup>	Crude HR (95% CI)	Adjusted HR <sup>a</sup> (95% CI)	P <sup>a</sup>
Age, 1-year increase	1.02 (0.99–1.05)	1.02 (1.00–01.05)	0.046	1.03 (0.99–1.06)	1.02 (0.99–1.05)	0.2
Histotypes, %						
Ductal carcinoma	1 (ref. cat.)			1 (ref. cat.)		
Lobular carcinoma	1.06 (0.52–2.18)			1.23 (0.55–2.71)		
Others	0.66 (0.36–1.21)			0.76 (0.38–1.53)		
Molecular classes, %						
Luminal A	1.07 (0.48–2.37)			1.18 (1.45–3.05)		
Luminal B	0.91 (0.41–1.99)			0.90 (0.35–2.33)		
HER2 <sup>+</sup>	1 (ref. cat.)			1 (ref. cat.)		
Triple negative	0.83 (0.30–2.36)			1.18 (0.38–3.67)		
HER2 expression	1.17 (0.67–2.04)			1.25 (0.65–2.38)		
Stage, 1-stage increase	2.74 (1.87–4.01)	2.83 (1.92–4.19)	<0.001	3.78 (2.29–6.24)	3.69 (2.23–6.11)	<0.001
Lymph node metastases	5.68 (2.77–11.7)			10.1 (3.61–28.4)		
IL30 expression in breast cancer cells (primary tumor)						
Negative	1 (ref. cat.)	1 (ref. cat.)	–	1 (ref. cat.)	1 (ref. cat.)	–
Weakly positive	0.78 (0.41–1.47)	0.91 (0.48–1.73)	0.8	0.66 (0.33–1.36)	0.92 (0.45–1.89)	0.8
Positive	0.67 (0.32–1.39)	0.64 (0.31–1.32)	0.2	0.61 (0.27–1.38)	0.74 (0.33–1.67)	0.5
Weakly positive or positive vs. negative	0.74 (0.41–1.33)	0.79 (0.44–1.43)	0.4	0.64 (0.33–1.24)	0.85 (0.44–1.64)	0.6
IL30 expression in BRCA-ILK						
Scanty	1 (ref. cat.)	1 (ref. cat.)	–	1 (ref. cat.)	1 (ref. cat.)	–
Distinct	1.64 (0.92–1.92)	1.31 (0.73–2.34)	0.4	1.97 (1.01–3.83)	1.86 (0.94–3.69)	0.08
Strong	1.72 (0.79–3.75)	0.95 (0.43–2.10)	0.9	2.37 (0.98–5.75)	1.60 (0.65–3.88)	0.3
Distinct or strong vs. scanty	1.66 (0.97–2.83)	1.19 (0.68–2.06)	0.6	2.07 (1.11–3.84)	1.77 (0.94–3.34)	0.08
IL30 expression in LN-ILK						
Scanty	1 (ref. cat.)	1 (ref. cat.)	–	1 (ref. cat.)	1 (ref. cat.)	–
Distinct	2.61 (1.24–5.47)	1.51 (0.69–3.30)	0.3	3.46 (1.40–8.54)	2.00 (0.79–5.07)	0.14
Strong	4.07 (1.99–8.35)	1.90 (0.88–4.10)	0.1	5.47 (2.31–13.0)	2.52 (1.03–6.13)	0.042
Distinct or strong vs. scanty	3.25 (1.67–6.32)	1.70 (0.83–3.46)	0.15	4.40 (1.95–9.95)	2.27 (0.98–5.27)	0.06

Abbreviation: Ref. cat., reference category.

<sup>a</sup>Cox proportional hazard analysis including 156 observations. With the exception of age and IL30, which were forced to entry, and lymph node metastasis, which was excluded because of multicollinearity with stage, only the covariates that were significant at univariate analyses were included. Six different models were fit, each including 1 of the 6 IL30 variables (IL30 expression in T, either using dummy variables or dichotomized; IL30 expression in T-ILK, either using dummy variables or dichotomized; IL30 expression in LN-ILK, either using dummy variables or dichotomized), with all other covariates remaining stable.

the hrIL30 treatment boosted expression of the oncogene that increases ERBB2 phosphorylation, namely GRB7 (4.5 times; ref. 16), but also of CSF1 (9.49 times) and, most of all, PTGS2/COX2 (14.46 times), which belongs to the set of genes that characterize and mediates breast cancer metastasis to the lung (17). A set of tumor suppressor genes, which includes PTEN (4.29 times; ref. 18), RARB (7.56 times; ref. 19), RASSF1 (4.46 times;

ref. 20), SLIT2 (5.26 times; ref. 21), and particularly TP73 (10.09 times; ref. 22) were consistently downmodulated.

**Locally administered hrIL30 boosts the expression of breast cancer-associated genes and promotes tumor growth *in vivo***

To assess whether and how IL30 may condition *in vivo* breast cancer microenvironment, MDA-MB-231 cells, which

**Figure 2.**

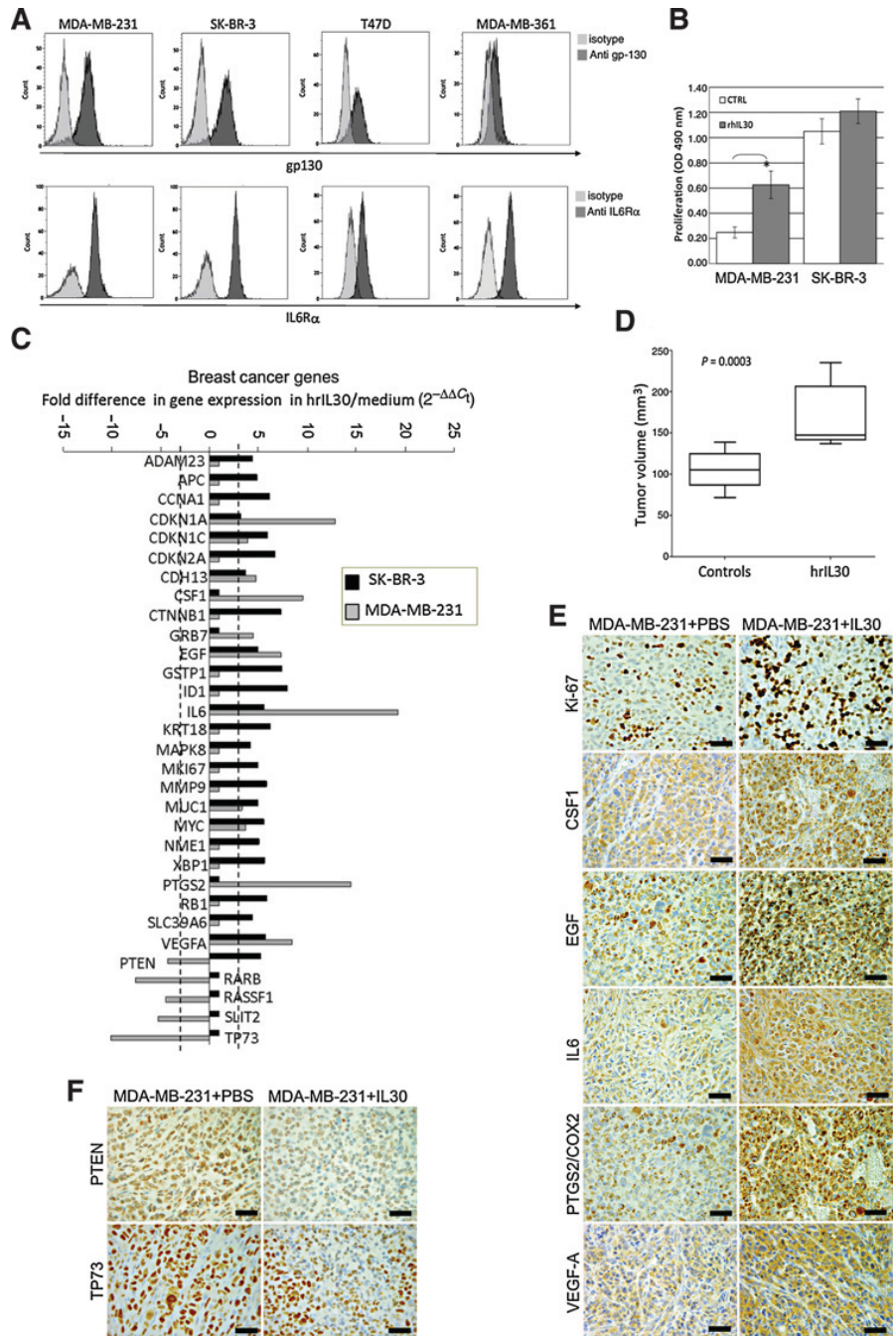
Expression of gp130 and IL6R $\alpha$  in hBRCA cell lines and their response to hrIL30 *in vitro* and *in vivo*.

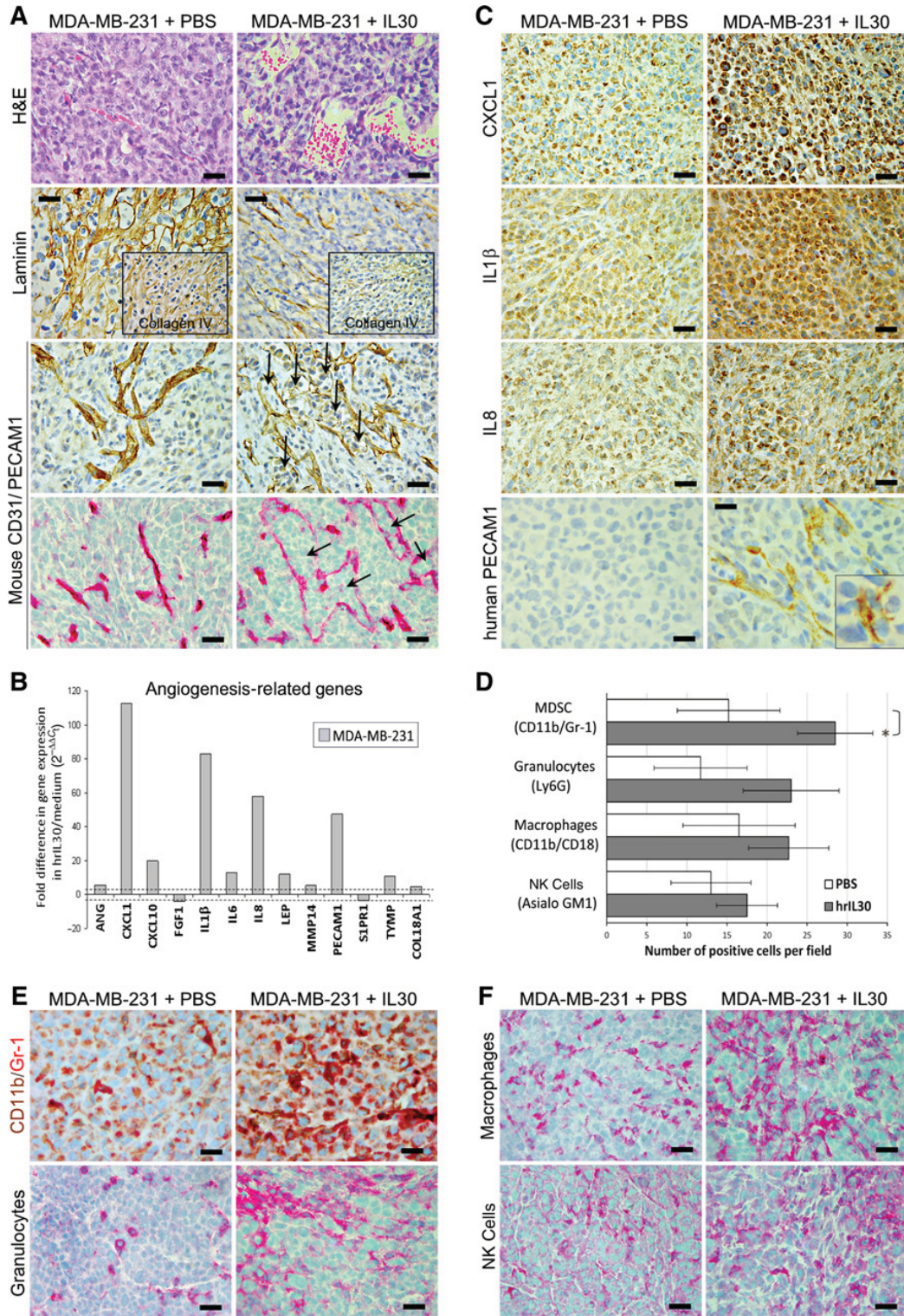
**A**, flow cytometric analyses of gp130 (top) and IL6R $\alpha$  (bottom) expression in hBRCA cells. Experiments were performed in triplicate. **B**, assessment of MDA-MB-231 and SK-BR-3 cell proliferation, 48 hours after hrIL30 treatment. Data are representative of three independent experiments.

**C**, fold differences of individual mRNAs between MDA-MB-231 and SK-BR-3 cells cultured with or without hrIL30. Pooled results  $\pm$  SD are from two experiments performed in duplicate. A significant threshold of 3-fold change in gene expression corresponded to  $P < 0.001$ .

**D**, volume of tumors developed in NSG mice orthotopically injected with MDA-MB-231 cells and treated with PBS or with biweekly doses of hrIL30 (1  $\mu$ g dose/mouse). Results are representative of three independent experiments.  $P = 0.0003$ .

**E**, cancer cell proliferation (Ki-67) and expression of CSF1, EGF, IL6, PTGS2/COX2, and VEGF-A in hrIL30-treated versus PBS-treated tumors ( $\times 400$ ). Scale bars, 30  $\mu$ m. **F**, expression of PTEN and TP73 in hrIL30-treated versus PBS-treated tumors ( $\times 400$ ). Scale bars, 30  $\mu$ m.





unlike SK-BR-3 cells, displayed tumorigenic capability in several strains of mice, were orthotopically injected in NSG mice and locally treated with hrIL30 or PBS (controls). Nineteen days after their implantation, MDA-MB-231 cells gave rise to tumors, which were significantly wider in mice treated with hrIL30 than in the controls [Fig. 2D;  $P = 0.0003$ , mean tumor volume (mtv) in IL30-treated mice vs. controls:  $169.8$  vs.  $105.4$  mm<sup>3</sup>] and were characterized by an increased cancer cell proliferation index (hrIL30-treated tumors:  $68.4\% \pm 9.0\%$  versus PBS-treated tumors:  $43.0\% \pm 8.5\%$ ;  $P < 0.05$ ) and an evident upregulation of CSF1, EGF, VEGF-A, most of all IL6 and PTGS2/COX2, along with a downregulation of PTEN and TP73 (Fig. 2E and F).

### hrIL30 regulates angiogenesis-related genes, favors abnormal vascular budding, and promotes endovascular tumor cell aggregates

Despite the ability of hrIL30 to upregulate IL6 and VEGF-A production by breast cancer cells, the number of intratumoral microvessels remained substantially unchanged in the treated tumors when compared with controls ( $9.7 \pm 3.6$  vessels per field in hrIL30-treated tumors vs.  $7.0 \pm 2.8$  in control tumors). Their features, however, were quite aberrant. They were mainly formed by ectatic endothelial branches, backed by a faint laminin network, and frequently clogged by wide tumor cell emboli (Fig. 3A). This observation led us to assess whether IL30 may affect the tumor vascular architecture by modulating tumor cell expression of angiogenesis-associated genes. Angiogenesis PCR-Array revealed a substantial upregulation of PECAM1, by 47.35 times, in hrIL30-treated breast cancer cells when compared with controls.

hrIL30 upregulation of IL6 (by 12.7 times) and VEGF-A (by 4.98 times), already revealed by breast cancer PCR-Array, was confirmed by angiogenesis gene expression analyses, whereas a variety of additional genes were upregulated including ANG (5.32 times), LEP (11.82 times), and TYMP (10.89 times). Specific antiangiogenesis genes were also upregulated, such as CXCL10/IP10 (19.73 times) and COL18A (4.44 times). Together with PECAM1, however, the most tightly upregulated genes were those coding for CXCL1 (112.47 times), IL1 $\beta$  (83.14 times), and IL8 (57.82 times). Expression of FGF1 and S1PR was slightly downmodulated by 3.99 and 3.51 times, respectively (Fig. 3B).

Immunohistochemical analyses of tumors from hrIL30-treated mice confirmed the ability of IL30 to induce PECAM1 expression on cancer cells (Fig. 3C) and boost their production of CXCL1, IL1 $\beta$ , and IL8. hrIL30 conditioned tumors were mildly enriched in CD11b<sup>+</sup>/CD18<sup>+</sup> macrophages, Ly6G neutrophils, and asialo GM1<sup>+</sup> natural killer (NK) cells, and consistently ( $P < 0.05$ ) infiltrated by myeloid CD11b<sup>+</sup>/Gr1<sup>+</sup> cells in comparison with controls (Fig. 3D-F).

### STAT1/STAT3 silencing hinders hrIL30-induced expression of critical tumor growth and progression factors in triple-negative hBRCA cells

Because the gp130 engagement activates the Janus family kinases and leads to the recruitment and phosphorylation of STAT1/3, we assessed phospho-STAT1 and phospho-STAT3 in hrIL30-treated versus control tumors and found they were both upregulated following treatment (Fig. 4A). We then knocked down, with specific siRNA, these transcription factors in MDA-MB-231 cells (Fig. 4B) to investigate their involvement in IL30-dependent boosting of the main tumor growth/progression mediators. Silencing of STAT3 substantially ( $P < 0.05$ ) hampered hrIL30-dependent expression of CXCL1 (lowered by 3.19 times) and CSF1 (by 3.14 times) and abolished IL1 $\beta$ , IL6, IL8, PTGS2/COX2, and MYC upregulation, whereas STAT1 knockdown heavily hindered IL8 (by 8.40 times) and PTGS2/COX2 (by 3.65 times) upregulation in MDA-MB-231 cells (Fig. 4C).

### IL30 promotes breast cancer cell migration and invasiveness and regulates matrix metalloproteases expression, stemness, and metastasis-associated genes

Because the endogenous expression of IL30 by LN-ILK, independently of whether lymph nodes were sites of metastasis, was closely associated with the development of lymph node metastasis, we next investigated the ability of IL30 to affect breast cancer cell migration and invasiveness, two processes required for metastasis. MDA-MB-231 cells displayed an increased ( $P < 0.05$ ) migration capability toward the cytokine conditioned media when compared with media alone and also revealed an increased invasion across the Matrigel-coated inserts (Fig. 4D and E).

Assessment of proteolytic enzymes in hrIL30-treated MDA-MB-231 cells, by angiogenesis PCR-Array, revealed a significant increase in the expression of MMP14 by 5.39 times, whereas the expression of ADAM23, CST6, CTSD, MMP2, MMP9, PLAUI, and PYCARD remained substantially unchanged. We next extended our analyses to additional sets of genes critically involved in cancer cell invasiveness and motility, namely, metastasis suppressors (*KISS1*, *PEBP1/RKIP*, *KAI1/CD82*, *MAP2K4*, *MAP2K7*, *NDRG1*; ref. 23), pluripotency and epithelial-to-mesenchymal transition (EMT) genes (*SNAI1*, *SNAI2*, *ZEB1*, *ZEB2*, *TWIST1*, *TWIST2*, *N-CADH*, *E-CADH*; ref. 24). hrIL30 treatment of MDA-MB-231 cells resulted in a significant downregulation of *KISS1* (by 5.03 times, at transcriptional level), which were confirmed *in vivo* by immunostaining (Fig. 4F). The expression of EMT transcription factors remained substantially unchanged, whereas within the pluripotency genes (*NOTCH1*, *OCT4A*, *SHH*, *KLF4*, *BMI1*, *CD44v6*, *YAP1*, *WWTR1*), expression of SONIC HEDGEHOG (SHH) was

### Figure 3.

Effects of hrIL30 treatments in breast cancer cells and xenograft. **A**, hematoxylin and eosin (H&E) and immunostainings revealed that microvessels supplying hrIL30-treated tumors were ectatic and backed by a faint laminin and collagen (insets) network. Anti-mouse CD31 immunostaining in both paraffin-embedded and frozen sections showed vessels clogged by tumor cell emboli (arrows;  $\times 400$ ). Scale bars, 30  $\mu$ m. **B**, fold differences of individual mRNAs between MDA-MB-231 cells cultured with or without 200 ng/mL hrIL30. Pooled results  $\pm$  SD are from two experiments performed in duplicate. A significant threshold of 3-fold change in gene expression corresponded to  $P < 0.001$ . **C**, expression of CXCL1, IL1 $\beta$ , IL8, and PECAM1 (inset at  $\times 1,000$ ) in hrIL30-treated versus PBS-treated tumors ( $\times 400$ ). Scale bars, 30  $\mu$ m. (Anti-hPECAM1 staining;  $\times 630$ ). Scale bars, 20  $\mu$ m. **D**, immune cell infiltrates in hrIL30-treated versus PBS-treated tumors. Results are expressed as mean  $\pm$  SD of positive cells/field evaluated by immunohistochemistry. \*, values significantly ( $P < 0.05$ ) different from corresponding values in control tumors. **E**, CD11b<sup>+</sup>/Gr1<sup>+</sup> and granulocyte infiltrates in hrIL30-treated versus PBS-treated tumors ( $\times 400$ ). Scale bars, 30  $\mu$ m. **F**, macrophage and NK cell infiltrates in hrIL30-treated versus PBS-treated tumors ( $\times 400$ ). Scale bars, 30  $\mu$ m.



consistently upregulated by hrIL30 treatment at the transcriptional level, *in vitro* (10.09 times), and at the protein level, *in vivo*, as revealed by immunohistochemical analyses of IL30-treated versus control tumors (Fig. 4F).

## Discussion

The awareness that the microenvironment is a critical determinant of tumor behavior (1) urges the discovery of signaling molecules upstream the inflammatory cascade driving cancer behavior, clinical outcome, and response to therapy (2, 3).

We identify IL30 as a cytokine able to condition, in an autocrine or paracrine manner, gene expression profile, at times the viability, motility, and invasiveness of breast cancer cells and to generate an inflammatory and prometastatic milieu supporting tumor growth and progression.

Although IL30 expression by both breast cancer and infiltrating immune cells is tightly associated with triple-negative and HER2<sup>+</sup> subtypes, suggesting this cytokine as part of a worst prognosis signature, strong IL30 production by LN-ILK is linked with metastasization and advanced disease stage, independently of the molecular subtype of breast cancer. These observations, which support the previously proposed protumoral function of IL30 (10–12), led us to gain further insight into the molecular and cellular mechanisms involved.

Association of IL30 expression by monocytes, macrophages and myeloid-derived suppressor cells in cancer draining lymph nodes with disease recurrence at univariate analysis, and with mortality at the multivariate analysis, candidates this cytokine as a novel independent predictor of poor clinical outcome in breast cancer and corroborates the prometastatic role of myeloid cells (25). These cells, probably attracted by CSF1, IL8, and CXCL1, which are considerably upregulated in cancer cells by IL30 stimulation, may function as both target and source of IL30 and as a main ally in orchestrating cancer cell migration and homing at distant site.

In breast cancer, overexpression of CSF1 and its receptor correlates with poor prognosis. CSF1 promotes breast cancer malignancy and invasiveness and with the cooperation of EGF, also upregulated in cancer cells by IL30, may lead to a prominent myeloid cell infiltration (26, 27) in IL30 conditioned tumors.

IL8, which increases more than 50 times in the IL30-treated triple-negative breast cancer cells, stimulates migration, invasion, intravasation, and favors metastasization (28). It has been recently identified as the single most important risk factor of poor prognosis in the triple-negative breast cancers (29) and the most upregulated within the genes included in the "invasion gene signature." Along with IL6, it is involved in the self-seeding of breast cancer, which is relevant for tumor growth and breeding of metastatic cell progenies (30). Boosted by IL30, with which it shares both receptor chains (9), IL6 production by cancer cells may act in an autocrine or paracrine manner to promote tumor growth (30). Aberrantly elevated IL6 is associated with a poor prognosis in breast cancer (31).

GRO1/CXCL1, which increases more than a 100-fold in IL30-treated triple-negative breast cancer cells, is implicated in invasion and infiltration. Its expression, along with that of PTGS2/COX2, also strongly induced by IL30, is associated in breast tumors with priming of breast cancer cells for seeding of the lungs (17) and is predictive of poor prognosis. It has

been recently reported to be central, through the recruitment of tumor feeding myeloid cells, to the mechanism linking chemoresistance to the resumption of tumor growth and development of metastasis (32). The substantial production of CXCL1 as well as that of IL6 and IL1 $\beta$  (33, 34) may account for the prominent CD11b<sup>+</sup>/Gr1<sup>+</sup> myeloid cell infiltrate of IL30-treated tumors, although a direct chemotactic effect of IL30 cannot be ruled out at present.

Overexpression of IL1 $\beta$  has been described in solid tumors, including breast cancer. Greatly upregulated by IL30, it is an upstream cytokine, which initiates and propagates inflammation, induces stabilization of IL8mRNA and regulates migration of MDA-MB-231 cells (35).

Knockdown of STAT3 in these cells abolishes the ability of IL30 to induce IL1 $\beta$ , IL6, IL8, PTGS2/COX2, and MYC expression and heavily hampers CXCL1 and CSF1 upregulation, thus confirming these genes as STAT3 targets also in this system, whereas STAT1 silencing hinders IL30-mediated upregulation of IL8 and PTGS2/COX2 (36, 37). Thus, most of the protumoral effects of IL30 seem to be essentially mediated by STAT1/3 phosphorylation and activation, which clearly increase in IL30 conditioned tumor.

The close association between IL30 expression and lymph node metastasization in patients with breast cancer, most probably rests on both the ability of IL30 to directly favor cancer cell migration and invasion, possibly by the upregulation of MMP14 (38), and the prometastatic effects of the above-described second-level cytokines and chemokines. *In vitro* and *in vivo* downregulation of KISS1 in triple-negative breast cancer cells can also take part in the IL30-driven prometastatic program, although contrasting data on the metastasis suppression function of KISS1-derived peptides/KISS1R axis have been reported in breast cancer (39).

In both triple-negative and HER2<sup>+</sup> cell lines, IL30 upregulates the proto-oncogenes MYC and MUC1, which are involved in multiple pathways that control cell growth, proliferation, metabolism, and survival (40, 41) and also up-regulates tumor suppressors like CDKN1A/p21 (13), CDKN1C/p57 (14), and CDH13 (15), thus suggesting a delicate balance of cell death and proliferation. However, the higher proliferative activity observed in IL30 conditioned versus control tumors proves that the multiple signaling pathways triggered by the cytokine results, as a whole, in tumor growth and progression. In addition, at least in the triple-negative tumor, IL30 substantially upregulates SHH, which accelerates MDA-MB-231 cell proliferation (42) and is fundamental in the maintenance of a putative cancer stem cell compartment along with MYC, which is also upregulated by IL30 (43, 44). Moreover, IL30 downmodulates a set of critical tumor suppressors such as PTEN (18), RARB (19), RASSF1 (20), SLIT2 (21), and particularly TP73 (22), which lead to alterations in the cell-cycle regulation and a defective apoptotic response.

Within the breast cancer genes whose expression is substantially increased by IL30 treatment, leptin, an adipocyte-derived adipokine, has been recently recognized to be fundamental in linking obesity and cancer (45). MDA-MB-231 cells, as most breast cancer cell lines, are endowed with the leptin receptor and respond to leptin by upregulating p-STAT3, Bcl-x<sub>L</sub>, cyclin D1, and proliferating cell nuclear antigen (PCNA), thus increasing their proliferation (45). Leptin promotes mammary tumor growth from the early stage, by supporting cancer stem cells from survival

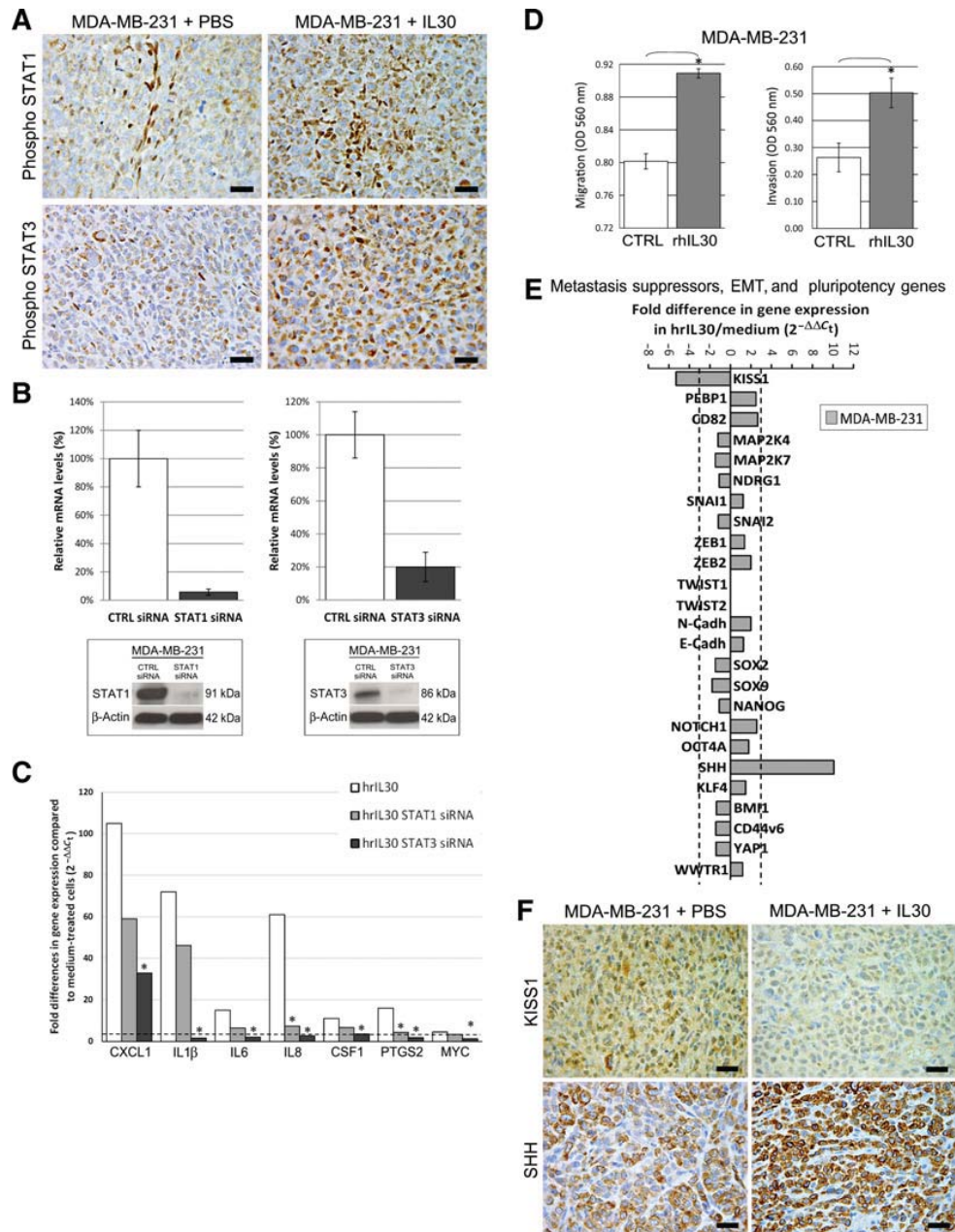


**Figure 4.**

Role of STAT1 and STAT3 in hrIL30 induction of tumor growth/progression mediators in hBRCA cells. Migration and invasion ability and expression of stemness and metastasis-associated genes in human breast cancer cells treated with hrIL30. **A**, immunohistochemistry showing phospho-STAT1 and phospho-STAT3 staining in hrIL30-treated versus PBS-treated tumors ( $\times 400$ ). Scale bars, 30  $\mu\text{m}$ . **B**, silencing of STAT1 (94%) and STAT3 (80%) in MDA-MB-231 cells, assessed by real-time RT-PCR, and confirmed at protein level by Western blotting.  $\beta$ -Actin was used as a loading control. \*,  $P < 0.05$  by Student  $t$  test compared with CTRL cells. **C**, fold differences of individual mRNAs between STAT1 siRNA- or STAT3 siRNA- or CTRL siRNA-transfected MDA-MB-231 cells cultured with hrIL30 and CTRL siRNA-transfected MDA-MB-231 cells cultured without hrIL30. Results from the latter are comparable to those obtained from untransfected cells. Pooled results  $\pm$  SD are from two experiments performed in duplicate. A significant threshold of 3-fold change in gene expression corresponded to  $P < 0.001$ . \*,  $P < 0.05$  by Student  $t$  test compared with CTRL siRNA-transfected MDA-MB-231 cells cultured with hrIL30. **D**, number of migrating and invading MDA-MB-231 cells was significantly increased 48 hours after hrIL30 treatment. Experiments were performed in triplicate. Results were expressed as mean  $\pm$  SD. \*,  $P < 0.05$  by Student  $t$  test compared with control cells. **E**, differences of individual mRNAs between MDA-MB-231 cells cultured for 48 hours with or without 200 ng/mL hrIL30. Pooled results  $\pm$  SD from two experiments performed in duplicate. A significant threshold of 3-fold change in gene expression corresponded to  $P < 0.001$ . **F**, KISS1 and SHH expression in hrIL30-treated versus PBS-treated tumors ( $\times 400$ ). Scale bars, 30  $\mu\text{m}$ .

to metastasization and by boosting cancer cells for proliferation, migration, and invasion.

In addition, IL30 upregulates specific proangiogenesis mediators such as ANG, TYMP, VEGF-A, COL18A, and in a remarkable way, the antiangiogenic chemokine CXCL10 (46). Subversion of this complex angioregulatory gene network results *in vivo* in a prominent but not significantly increased vascularity in IL30-treated tumors when compared with controls, from which they substantially differ by the abnormally dilated vascular branches endowed with a weakened collagen and laminin backbone favoring this widespread vascular dilation. Ectatic vessels are frequently clogged by tumor cell emboli, which may result from the short-circuiting step of encircling vasculogenesis rather than from the classic step of vascular invasion (47). PECAM1 expression by IL30-treated cancer cells might select for cancer clusters that easily engage endothelial cells in encircling vasculogenesis (47). PECAM1 mediates tumor cell–tumor cell homotypic adhesion as well as tumor cell–platelet–endothelial cell interactions (48), which can shape intravascular tumor cell aggregates within IL30-treated tumors and prepare for cancer cell dissemination (49).

Although further studies are needed to fully understand the multifaceted role of IL30 in human breast cancer biology, this work reveals for the first time its implications in breast carcinogenesis showing that (i) directly and/or by subverting multiple oncogenes and tumor suppressor genes, IL30 favors cancer cell proliferation, migration, and dissemination; (ii) it may boost cancer cell expression of cytokines and chemokines, which promote myeloid cell recruitment and tumor progression; (iii) IL30 is expressed in most breast cancers and associated with triple-negative and HER2<sup>+</sup> subtypes; (iv) IL30 expression by BRCA-ILK and LN-ILK correlates with breast cancer stage and, more importantly, high level of IL30 in breast

cancer draining lymph nodes is an independent predictor of poor clinical outcome.

Identification of IL30 in breast and draining lymph nodes may provide a new prognostic tool and target for a tailored breast cancer therapy in the emerging era of personalized medicine.

### Disclosure of Potential Conflicts of Interest

No potential conflicts of interest were disclosed.

### Authors' Contributions

**Conception and design:** E. Di Carlo

**Development of methodology:** I. Airoldi, C. Cocco, D. Angelucci, S. Di Meo, S. Esposito, M. Bertolotto

**Acquisition of data (provided animals, acquired and managed patients, provided facilities, etc.):** C. Cocco, D. Ribatti, C. Natoli

**Analysis and interpretation of data (e.g., statistical analysis, biostatistics, computational analysis):** I. Airoldi, C. Sorrentino, L. Manzoli, D. Ribatti

**Writing, review, and/or revision of the manuscript:** L. Manzoli, C. Natoli, E. Di Carlo

**Administrative, technical, or material support (i.e., reporting or organizing data, constructing databases):** L. Iezzi

**Study supervision:** L. Manzoli, E. Di Carlo

### Grant Support

This work was supported by grants from the Associazione Italiana Ricerca sul Cancro (IG-13134 to E. Di Carlo and IG-13018 to I. Airoldi) and by the Italian Ministry of Health, Ricerca Finalizzata (RF-2013-02357552 to E. Di Carlo and RF-2010-2308270 to I. Airoldi). C. Cocco was recipient of a fellowship from Fondazione Umberto Veronesi.

The costs of publication of this article were defrayed in part by the payment of page charges. This article must therefore be hereby marked *advertisement* in accordance with 18 U.S.C. Section 1734 solely to indicate this fact.

Received January 19, 2016; revised July 8, 2016; accepted August 4, 2016; published OnlineFirst August 22, 2016.

### References

- Torre LA, Bray F, Siegel RL, Ferlay J, Lortet-Tieulent J, Jemal A. Global cancer statistics, 2012. *CA Cancer J Clin* 2015;65:87–108.
- Sørlie T, Perou CM, Tibshirani R, Aas T, Geisler S, Johnsen H, et al. Gene expression patterns of breast carcinomas distinguish tumor subclasses with clinical implications. *Proc Natl Acad Sci U S A* 2001;98:10869–74.
- Rothschild E, Banerjee D. Subverting subversion: a review on the breast cancer microenvironment and therapeutic opportunities. *Breast Cancer (Auckl)* 2015;9:7–15.
- Pflanz S, Timans JC, Cheung J, Rosales R, Kanzler H, Gilbert J, et al. IL-27, a heterodimeric cytokine composed of EB13 and p28 protein, induces proliferation of naive CD4<sup>+</sup> T cells. *Immunity* 2002;16:779–90.
- Cocco C, Di Carlo E, Zupo S, Canale S, Zorzoli A, Ribatti D, et al. Complementary IL-23 and IL-27 anti-tumor activities cause strong inhibition of human follicular and diffuse large B-cell lymphoma growth *in vivo*. *Leukemia* 2012;26:1365–74.
- Di Carlo E, Sorrentino C, Zorzoli A, Di Meo S, Tupone MG, Ognio E, et al. The antitumor potential of interleukin-27 in prostate cancer. *Oncotarget* 2014;5:10332–41.
- Liu X, Wang Z, Ye N, Chen Z, Zhou X, Teng X, et al. A protective role of IL-30 via STAT and ERK signaling pathways in macrophage-mediated inflammation. *Biochem Biophys Res Commun* 2013;435:306–12.
- Stumhofer JS, Tait ED, Quinn WJ III, Hosken N, Spudy B, Goenka R, et al. A role for IL-27p28 as an antagonist of gp130-mediated signaling. *Nat Immunol* 2010;11:1119–26.
- Garbers C, Spudy B, Aparicio-Siegmund S, Waetzig GH, Sommer J, Hölscher C, et al. An interleukin-6 receptor-dependent molecular switch mediates signal transduction of the IL-27 cytokine subunit p28 (IL-30) via a gp130 protein receptor homodimer. *J Biol Chem* 2013;288:4346–54.
- Shimozato O, Sato A, Kawamura K, Chiyo M, Ma G, Li Q, et al. The secreted form of p28 subunit of interleukin (IL)-27 inhibits biological functions of IL-27 and suppresses anti-allogeneic immune responses. *Immunology* 2009;128:e816–25.
- Di Meo S, Airoldi I, Sorrentino C, Zorzoli A, Esposito S, Di Carlo E. Interleukin-30 expression in prostate cancer and its draining lymph nodes correlates with advanced grade and stage. *Clin Cancer Res* 2014;20:585–94.
- Di Carlo E. Interleukin-30: A novel microenvironmental hallmark of prostate cancer progression. *Oncoimmunology* 2014;3:e27618.
- Abbas T, Dutta A. p21 in cancer: intricate networks and multiple activities. *Nat Rev Cancer* 2009;9:400–14.
- Guo H, Tian T, Nan K, Wang W. p57: A multifunctional protein in cancer (Review). *Int J Oncol* 2010;36:1321–9.
- Andreeva AV, Kutuzov MA. Cadherin 13 in cancer. *Genes Chromosomes Cancer* 2010;49:775–90.
- Pias S, Peterson TA, Johnson DL, Lyons BA. The intertwining of structure and function: proposed helix-swapping of the SH2 domain of Grb7, a regulatory protein implicated in cancer progression and inflammation. *Crit Rev Immunol* 2010;30:299–304.
- Minn AJ, Gupta GP, Siegel PM, Bos PD, Shu W, Giri DD, et al. Genes that mediate breast cancer metastasis to lung. *Nature* 2005;436:518–24.
- Song MS, Salmena L, Pandolfi PP. The functions and regulation of the PTEN tumour suppressor. *Nat Rev Mol Cell Biol* 2012;13:283–96.

19. Liu X, Giguère V. Inactivation of RAR $\beta$  inhibits Wnt1-induced mammary tumorigenesis by suppressing epithelial-mesenchymal transitions. *Nucl Recept Signal* 2014;12:e004.
20. Buhmeida A, Merdad A, Al-Maghrabi J, Al-Thobaiti F, Ata M, Bugis A, et al. RASSF1A methylation is predictive of poor prognosis in female breast cancer in a background of overall low methylation frequency. *Anticancer Res* 2011;31:2975–81.
21. Qin F, Zhang H, Ma L, Liu X, Dai K, Li W, et al. Low Expression of Slit2 and Robo1 is Associated with Poor Prognosis and Brain-specific Metastasis of Breast Cancer Patients. *Sci Rep* 2015;5:14430.
22. Maas AM, Bretz AC, Mack E, Stiewe T. Targeting p73 in cancer. *Cancer Lett* 2013;332:229–36.
23. Smith SC, Theodorescu D. Learning therapeutic lessons from metastasis suppressor proteins. *Nat Rev Cancer* 2009;9:253–64.
24. Voutsadakis IA. The network of pluripotency, epithelial-mesenchymal transition, and prognosis of breast cancer. *Breast Cancer (Dove Med Press)* 2015;7:303–19.
25. Kitamura T, Qian BZ, Pollard JW. Immune cell promotion of metastasis. *Nat Rev Immunol* 2015;15:73–86.
26. Patsialou A, Wyckoff J, Wang Y, Goswami S, Stanley ER, Condeelis JS. Invasion of human breast cancer cells *in vivo* requires both paracrine and autocrine loops involving the colony-stimulating factor-1 receptor. *Cancer Res* 2009;69:9498–506.
27. Goswami S, Sahai E, Wyckoff JB, Cammer M, Cox D, Pixley FJ, et al. Macrophages promote the invasion of breast carcinoma cells via a colony-stimulating factor-1/epidermal growth factor paracrine loop. *Cancer Res* 2005;65:5278–83.
28. Patsialou A, Wang Y, Lin J, Whitney K, Goswami S, Kenny PA, et al. Selective gene-expression profiling of migratory tumor cells *in vivo* predicts clinical outcome in breast cancer patients. *Breast Cancer Res* 2012;14:R139.
29. Rody A, Karn T, Liedtke C, Pusztai L, Ruckhaeberle E, Hanker L, et al. A clinically relevant gene signature in triple negative and basal-like breast cancer. *Breast Cancer Res* 2011;13:R97.
30. Kim MY, Oskarsson T, Acharyya S, Nguyen DX, Zhang XH, Norton L, et al. Tumor self-seeding by circulating cancer cells. *Cell* 2009;139:1315–26.
31. Dethlefsen C, Højfeldt G, Hojman P. The role of intratumoral and systemic IL-6 in breast cancer. *Breast Cancer Res Treat* 2013;138:657–64.
32. Acharyya S, Oskarsson T, Vanharanta S, Malladi S, Kim J, Morris PC, et al. A CXCL1 paracrine network links cancer chemoresistance and metastasis. *Cell* 2012;150:165–78.
33. Oh K, Ko E, Kim HS, Park AK, Moon HG, Noh DY. Transglutaminase 2 facilitates the distant hematogenous metastasis of breast cancer by modulating interleukin-6 in cancer cells. *Breast Cancer Res* 2011;13:R96.
34. Tu S, Bhagat G, Cui G, Takaishi S, Kurt-Jones EA, Rickman B, et al. Over-expression of interleukin-1beta induces gastric inflammation and cancer and mobilizes myeloid-derived suppressor cells in mice. *Cancer cell* 2008;14:408–19.
35. Naldini A, Filippi I, Miglietta D, Moschetta M, Giavazzi R, Carraro F. Interleukin-1 $\beta$  regulates the migratory potential of MDAMB231 breast cancer cells through the hypoxia-inducible factor-1 $\alpha$ . *Eur J Cancer* 2010;46:3400–8.
36. Pensa S, Regis G, Boselli D, Novelli F, Poli V. STAT1 and STAT3 in tumorigenesis: two sides of the same coin? In: Bell HR Jr, editor. *JAK-STAT pathway in disease*. Abingdon-on-Thames, England: Taylor & Francis Group; 2009.
37. Carpenter RL, Lo HW. STAT3 target genes relevant to human cancers. *Cancers* 2014;6:897–925.
38. Devy L, Huang L, Naa L, Yanamandra N, Pieters H, Frans N, et al. Selective inhibition of matrix metalloproteinase-14 blocks tumor growth, invasion, and angiogenesis. *Cancer Res* 2009;69:1517–26.
39. Cvetković D, Babwah AV, Bhattacharya M. Kisspeptin/KISS1R system in breast cancer. *J Cancer* 2013;4:653–61.
40. Varlakhanova NV, Knoepfler PS. Acting locally and globally: Myc's ever-expanding roles on chromatin. *Cancer Res* 2009;69:7487–90.
41. Kufe DW. MUC1-C oncoprotein as a target in breast cancer: activation of signaling pathways and therapeutic approaches. *Oncogene* 2013;32:1073–81.
42. Ge X, Lyu P, Gu Y, Li L, Li J, Wang Y, et al. Sonic hedgehog stimulates glycolysis and proliferation of breast cancer cells: Modulation of PFKFB3 activation. *Biochem Biophys Res Commun* 2015;464:862–8.
43. Kasper M, Jaks V, Fiaschi M, Tofgård R. Hedgehog signalling in breast cancer. *Carcinogenesis* 2009;30:903–11.
44. Laurenti E, Wilson A, Trumpp A. Myc's other life: stem cells and beyond. *Curr Opin Cell Biol* 2009;21:844–54.
45. Andò S, Barone I, Giordano C, Bonfigliolo D, Catalano S. The multifaceted mechanism of leptin signaling within tumor microenvironment in driving breast cancer growth and progression. *Front Oncol* 2014;4:340.
46. Angiolillo AL, Sgadari C, Taub DD, Liao F, Farber JM, Maheshwari S, et al. Human interferon-inducible protein 10 is a potent inhibitor of angiogenesis *in vivo*. *J Exp Med* 1995;182:155–62.
47. Mahooti S, Porter K, Alpaugh ML, Ye Y, Xiao Y, Jones S, et al. Breast carcinomatous tumoral emboli can result from encircling lymphovascularogenesis rather than lymphovascular invasion. *Oncotarget* 2010;1:131–47.
48. Tang DG, Chen YQ, Newman PJ, Shi L, Gao X, Diglio CA, et al. Identification of PECAM-1 in solid tumor cells and its potential involvement in tumor cell adhesion to endothelium. *J Biol Chem* 1993;268:22883–94.
49. Tsoi DT, Rowsell C, McGregor C, Kelly CM, Verma S, Pritchard KI. Disseminated tumor embolism from breast cancer leading to multiorgan failure. *J Clin Oncol* 2010;28:e180–3.